

Leveraging Bat Algorithm with Rough Neutrosophic Soft Set for Enhanced Oral Cancer Detection and Classification

Arwa Darwish Alzughaibi¹, Ebtesam Al-Mansor^{2,*}

¹ Applied college, Taibah University, Madinah, Saudi Arabia;
² Computer Sciences Department, Applied College, Najran University, Najran 66462, Saudi Arabia Emails: Azughaibi@taibahu.edu.sa; ehmalmansoor@nu.edu.sa

Abstract

Neutrosophic soft sets (NSS) are highly effective in representing neutral uncertain data. NSS model attracts several authors because it has huge range of applications in several areas such as decision-making, data analysis, smoothness of functions, probability theory, measurement theory, predicting, and operations research. Oral squamous cell carcinoma (OSCC) is the most general tumor around the world and its occurrence is on the increase in several populations. Early diagnosis plays vital role in improving diagnosis, treatment outcomes and survival rates. Although the new developments in understanding molecular mechanisms, late analysis and the implementation of precision medicine for OSCC patients continue to present problems. Early diagnosis and detection can support doctors in offering optimum patient care and effectual treatment. In recent years, the execution of several machine-learning (ML) approaches in cancer analysis has provided valuable insights, facilitating more effective and precise treatment decision-making. Oral Cancer screening can progress with the execution of artificial intelligence (AI) approaches. AI offers support to the oncology region by correctly examining a huge database in many imaging modalities. This article develops a Bat Algorithm with Rough Neutrosophic Soft Set for Oral Cancer Diagnosis (BARNSS-OCD) technique. The main intention of the BARNSS-OCD technique is to exploit deep learning (DL) model for enhanced identification of OC. In the BARNSS-OCD technique, median filtering (MF) is used for image pre-processing and the feature extraction takes place using deep convolutional neural network (DCNN) model. In addition, bat algorithm (BA) is used for the hyperparameter selection of the DCNN model. For OC detection process, the BARNSS-OCD technique applies RNSS model. To exhibit the improved performance of the BARNSS-OCD technique, a sequence of experiments is involved. The simulation outcomes indicate that the BARNSS-OCD technique gains better performance compared to other DL models

Keywords: Oral Cancer; Neutrosophic Soft Set; Bat Algorithm; Oral Squamous Cell Carcinoma; Deep Learning

1. Introduction

Oral cancer (OC) is a kind of pharyngeal cancer that mostly affects the lips, tongue, throat, and mouth [1]. The mortality rate of OC is comparatively higher, with around 11,580 deaths in 2023. In comparison to women, men are at higher risk of developing oral cancer, and the risk rises with age [2]. Early treatment and recognition of OC are significant for better performance. Some anxiety problems can occur in different ways in our daily life [3]. Therefore, the two most important aspects in controlling the decision making procedure are the most accurate representation of the problem of uncertainty and obtaining accurate results when solving the problem [4]. Researchers have developed a variety of mathematical approaches that can provide the most accurate results. Though fuzzy sets were the 1st mathematical models presented from the domain, it is a very successful theory [5]. It is well-known that the theories utilized for expressing uncertainty have a logic set consisting of three independent components characterized by truth, uncertainty, and false membership. It is a fact. Therefore, the biggest advantage of this mathematical model is that it can manage undefined data that cannot be handled by fuzzy and intuitive fuzzy sets [6].

Deep learning (DL)is a branch of AI that established utilizing NNs [7]. NNs are nature-inspired programming algorithms that enable complex representations to augment pattern recognition from raw data [8]. These methods consist of several layers that transform an input database (medical imagery) into an output (diagnosis or diagnostic recommendation) but automatically learn higher-level features. DL is widely utilized in medical domains like diagnosis, and recognizing abnormalities in medical images, and has proven effectual in investigating difficult data [9]. Integrating DL technology into daily practice of medicine requires diagnostic efficiency comparable to that of specialized medical care [10]. Additionally, it should offer other benefits, such as ethical behavior, speed efficacy, lower costs, and increased accessibility.

This article develops a Bat Algorithm with Rough Neutrosophic Soft Set for Oral Cancer Diagnosis (BARNSS-OCD) technique. The main intention of the BARNSS-OCD technique is to exploit DL model for enhanced identification of OC. In the BARNSS-OCD technique, median filtering (MF) is used for image pre-processing and the feature extraction takes place using deep convolutional neural network (DCNN) model. In addition, BA is used for the hyperparameter selection of the DCNN model. For OC detection process, the BARNSS-OCD technique applies RNSS approach. The simulation values indicate that the BARNSS-OCD technique reaches better performance compared to other DL approaches.

2. Existing Works on OC Detection

Mira et al. [11] present a technique that depends on smartphone image analysis caused by DL approach. The centered rule process of image capture is provided in a fast and simple manner to develop high-resolution picture of mouth. A newly established DL network has been presented to evaluate OC analysis. Mohan et al. [12] examine a structure, OralNet, for OC recognition utilizing histopathology images. The research includes 4 phases such as image preprocessing, feature extractor employing deep and handcrafted system while removing important features from images utilizing DL and typical approaches, and feature reduction AHA. Huang et al. [13] introduce a new technique to detect OC utilizing an improved method of CNN. Although simple CNNs are extremely utilized for image classifier models, the combination of SOA and PSO methods in improving the CNN model, especially for OC recognition is a unique method that is offered. This technique also integrates advanced image processing approaches comprising data augmentation, noise reduction, and contrast enhancement.

Marzouk et al. [14] present AI with Deep TL-driven OC recognition and Classification Model (AIDTLOCCM). The presented AIDTL-OCCM approach contains fuzzy-based contrast enhancement system for executing data pre-processed. Afterward, the DenseNet169 technique can be deployed to create a valuable conventional of deep features. Additionally, the COA with AE approach can be executed for OC recognition and classification. Al Duhayyim et al. [15] develops a new CAD for OC utilizing Sailfish Optimizer with Fusion-based Classification (CADOC-SFOFC) algorithm. A fusion based feature extractor method has been implemented by utilizing VGGNet16 and ResNet approaches. Moreover, the feature vectors can fuse and accepted to the ELM technique for classifier method. Additionally, the SFO system can be employed for effectual parameter election of the ELM algorithm, so resulting in higher outcomes.

Khan and Asif [16] establish a new algorithm that integrates feature-level fusion systems for OC recognition. This method presents a new self-attention block as an initial element of the method. Moreover, the TL approaches can be deployed for feature fusion, especially EfficientNet-B0 and B1, popular for their efficiency in image classification tasks. A new self-attention block and leverage TL approaches can also be employed for extracting and combining important features. In [17], a new technique employing DL depends on meta-heuristic model is considered to offer a correct cancer analysis tool. During this case, the 3 pre-processing approaches can employ comprising noise reduction, Gamma correction, and data augmentation to improve the raw image qualities and enhance its numbers to offer sufficient data under the CNN training.

3. Materials and Methods

This article has presented a novel BARNSS-OCD technique. The main purpose of the BARNSS-OCD system is to utilize DL model for enhanced identification of OC. It contains four different kinds of procedures namely image preprocessing, DCNN based feature extractor, BA based parameter selection, and RNSS based OC detection. Fig. 1 represents the workflow of BARNSS-OCD system.

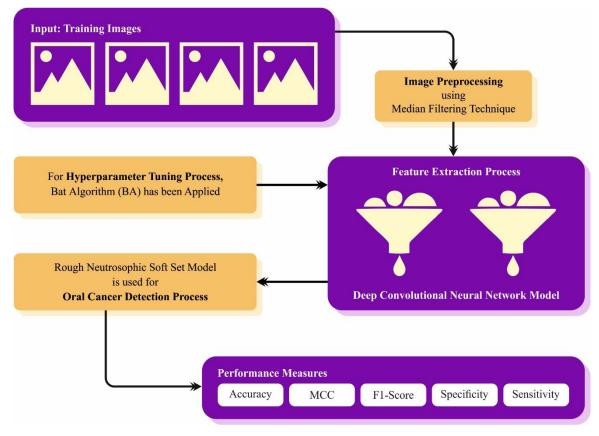


Figure 1: Workflow of BARNSS-OCD technique

A. Noise Elimination Process

Primarily, the BARNSS-OCD technique takes place when the MF is used for image pre-processing. MF is an extensively utilized image pre-processed approach intended to reduce noise while maintaining edges [18]. It mechanisms by exchanging each pixel value from the image with the median rate of the level of intensity in its adjacent region. This system is mostly effective at eradicating 'salt and pepper' noise, but random pixels can be set to maximum rates. MF is non-linear and supports preserving the sharpness of edges, achieving ideal of enhancing quality of image without blurring vital features.

B. Development of the DL Model Next

The feature extraction takes place using DCNN model. CNN is an extremely utilized NN structure in the domain of DL, initially planned to extract deep-level features without depending greatly on previous data for validation [19]. A standard CNN generally comprises layers like input, convolution, activation, pooling, FC, and output layers. In detail, the convolution layer is most fundamental CNN modules. Its key function is feature extractor. This procedure efficiently captures local features and patterns from the input data.

$$O^{l} = f\left(\sum_{i=1}^{N} X * K_{i} + b_{i}^{l}\right)$$

$$\tag{1}$$

whereas, X defines the input data, K_i implies the i^{th} convolution kernel, $f(\cdot)$ stands for the activation function, N denotes the convolution kernel counts utilized from the convolution layer, b_i^l implies the i^{th} deviation of feature maps of layer 1, an d^* defines the convolutional function.

This layer assists in reducing the computation load and decreases the count of parameters by discarding unnecessary instances in the database. This method is capably trained utilizing a BP method. Related to other shallow or DNNs, CNNs are well-known for their decreased parameter necessities, which leads them to a compelling optimal in DL structures. The formulation for computing CNN feature extractor was expressed as:

$$O^{l}(j) = \max_{(j-1)w \le t \le jw} \{X^{l-1}(t)\}$$
(2)

DOI: <u>https://doi.org/10.54216/IJNS.240405</u> Received: March 30, 2024 Revised: April 29, 2024 Accepted: May 26, 2024 73

whereas $O^{l}(j)$ denotes the outcomes of j^{th} pooled area of l layer, w implies the width of pooled area, and $X^{l-1}(t)$ indicates the pooled area. Fig. 2 represents the framework of DCNN.

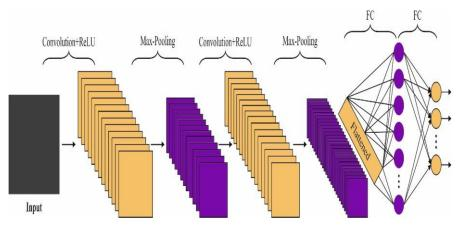


Figure 2: Architecture of DCNN

C. Model Parameter Selection

At this stage, BA is used for the hyperparameter selection of the DCNN model. The BA is an optimizer model stimulated by the echo location behavior of bats [20]. This technique captures the spirit of bats' refined biological sonar methods, transforming the dynamics of echo location and fight to a computation model proficient in penetrating global goals in difficult optimizer issues. During the BA, the population of simulated bats directs the space of solution, but every bat signifies a latent outcome. The bats utilize a mixture of echo location and a random walk (RW) to discover and utilize the space of solution efficiently. It is alter their echo location parameters like rate of pulse, frequency, and loudness to discover prey, equivalent to discovering the optimum outcomes in an assumed space of problem. This method uses the following formulation for upgrading the bats' locations and speeds:

$$f_i = f_{\min} + (f_{\max} - f_{\min})\beta \tag{3}$$

$$v_i(t+1) = v_i(t) + (X(t) - gbest)f_i$$
 (4)

$$x_i(t+1) = x_i(t) + v_i(t+1)$$
(5)

Whereas, f_i denotes the bat frequency *i* which ranges from f_{\min} to f_{\max} with β being a randomly generated number among zero and one. $v_i(t+1)$ signifies the bat velocity *i* at iteration t + 1, and *gbest* represents the global finest outcomes.

Furthermore, to perfect the bats' local exploration and exploitation ability, an RW is combined around the finest outcome that originated so far. It can be attained by adopting a bat's location utilizing the average volume A of every bat and the pulse emission value r, managing the searching near the optimal:

$$x_{new} = x_{gbest} + eA \tag{6}$$

Here, x_{new} signifies a novel solution produced by local search near the global finest location x_{gbest} , and e represents the randomly generated count represented from an even distribution. The A and r values reduce and upsurge correspondingly on the sequence of iterations, modifying the balance among exploitation and exploration dependent upon the proximity to the prey, i.e., the optimum performance.

The BA efficacy stems from its two techniques of global search, simplified by echo location-simulated action, and local search, improved by the RW dependent upon the loudness and pulse rate. This mixture permits the procedure to discover massive regions of the searching space and extensively search areas near the present finest solution.

The fitness election is main aspect regulatory the BA solution. The parameter election method comprises the encoding outcome to measure the effectiveness of candidate performances. During this case, the BA assumes that accuracy is a major condition to plan the FF that is written as:

$$Fitness = \max(P) \tag{7}$$

$$P = \frac{TP}{TP + FP} \tag{8}$$

In which, TP and FP stand for the true and false positive rates.

D. Classifier Architecture

Eventually, the BARNSS-OCD technique applies RNSS model for OC detection process. This section defines several approaches depending on fuzzy logic (FL) and Neutrosophic logic (NL) [21]. In later portions, these approaches can be utilized to classify data. FL is a multi-valued logic but the truth membership among is zero to one.

Definition1. Fuzzy set

A set of fuzzy X on U that is assumed as Universe is a function expressed as:

$$X = \{\mu_x(u)/u \colon u \in U\}$$
(9)

Where as $\mu_X : U \to [0, 1] \mu_X$ is named as membership function (MF) of X, the rate $\mu_X(u)$ is named as membership degree of $u \in U$. The value of membership lies among zero and one.

Definition2. Neutrosophic set (NS)

An NS A in U is assumed as items space and is represented by truth-MF T_A , an indeterminacy-MF I_A and falsity-MF F_A . An element appropriate to U is defined by u.

$$A = \{ < x, (T_A(x), I_A(x), F_A(x)) > : x \in U, T_A(u), I_A(u), F_A(u) \subseteq [0,1] \}$$
(10)

It is no constraints on the sum of $T_A(u)$, $I_A(u)$ and $F_A(u)$, therefore $-0 \le \sup T_A(u) + \sup I_A(u) + \sup F_A(u) \le 3$. The sum of 3 degrees takes any constraints as it lies among zero to three.

Definition3. Soft set (SS)

A SS F_A on U that is assumed that Universe, represented by a set appreciated function f_A demonstrating a mapping

$$f_A: E \to P(U)$$
 such that $f_A(x) = \emptyset$ if $x \in E - A$ (11)

whereas f_A is named as approximate function of SS F_A .

$$F_A = \{ (x, f_A(x)) : x \in E, f_A(x) = \emptyset \text{ if } x \in E - A$$
(12)

E implies the parameter set that defines the features of *U* and $A \in E$. The subscript *A* in f_A signifies that f_A is estimated purpose of F_A and is named as *x*-component of SS to all the $x \in E$.

Definition4. Neutrosophic SS (NSS)

Assume that U be a universe, N(U) refers to the set of every NS on U, E implies the parameter set that defines the elements of U. N on U refers the set demonstrated by a set appreciated function f_N signifying mapping

$$f_N: E \to N(U)$$
 such that $f_N(x) = \emptyset$ if $x \in E - A$ (13)

In which, f_N is named as approximate function of N.

$$N = \{ (x, f_N(x)) : x \in E, f(x) = \emptyset \text{ if } x \in E - A \}$$
(14)

Definition5. Rough NS (RNS)

Assume U exits a Universe of non-null rates and R is some equivalent connection on U. Let F be some NS in U with its belongings, uncertainty, and non-belonginess purpose. The low and high calculations of F from the estimate (U,R) that is defined by and $\overline{N}(F)$ are expressed as:

$$\underline{N}(F) = \{ \langle x, \mu_{\underline{N}(F)}(x), v_{\underline{N}(F)}(x), \omega_{\underline{N}(F)}(x) \rangle | y \in [x]_R, x \in U \}$$
(15)

$$\overline{N}(F) = \{ \langle x, \mu_{\overline{N}(F)}(x), \nu_{\overline{N}(F)}(x), \omega_{\overline{N}(F)}(x) \rangle | y \in [x]_R, x \in U \}$$
(16)

whereas

DOI: <u>https://doi.org/10.54216/IJNS.240405</u> Received: March 30, 2024 Revised: April 29, 2024 Accepted: May 26, 2024 75

$$\mu_{\underline{N}(F)}(x) =^{\wedge}_{y \in [x]_R} \mu_F(y), v_{\underline{N}(F)}(x) =^{\vee}_{y \in [x]_R} v_F(y), \omega_{\underline{N}(F)}(x) =^{\vee}_{y \in [x]_R} \omega_F(y)$$
(17)

$$\mu_{\overline{N}(F)}(x) =_{y \in [x]_R}^{\vee} \mu_F(y), \nu_{\overline{N}(F)}(x) =_{y \in [x]_R}^{\wedge} \nu_F(y), \omega_{\overline{N}(F)}(x) =_{y \in [x]_R}^{\wedge} \omega_F(y)$$
(18)

In which, mean min and max functions. The pair $(\underline{N}(F), \overline{N}(F))$ is named rough NS in (U,R). R refers to the equivalent connection on U.

Definition6. RNSS

They present a novel approach to Neutrosophic rough SS by integrating the NSS model and rough NS. RNSS offers low and up approximations for all classes.

Let *U* be some set of buildings and *E* implies the parameter sets. All the parameters is a Neutrosophic word. Assume $E = \{wooden, expensive, beautiful, cheap\}$. To determine a NSS, there is require to point out wooden buildings, costly buildings, etc. Assume there are 3 buildings from the universe *U* provided by $U = \{b1, b2, b3\}$ and parameter sets $A = \{e1, e2, e3, e4\}$ whereas e1 signifies the wooden, e2 implies the expensive, etc.

$$F(wooden) = \{ < b1, 0.6, 0.3, 0.4 >, < b2, 0.4, 0.6, 0.6 >, < b3, 0.6, 0.4, 0.2 > \},\$$

$$F(expensive) = \{ < b1, 0.7, 0.4, 0.5 >, < b2, 0.6, 0.2, 0.4 >, < b3, 0.7, 0.4, 0.3 > \},$$

 $F(beautiful) = \{ < b1, 0.8, 0.2, 0.1 >, < b2, 0.6, 0.7, 0.6 >, < b3, 0.8, 0.4, 0.3 > \},\$

$$F(cheap) = \{ < b1, 0.8, 0.2, 0.7 >, < b2, 0.4, 0.6, 0.4 >, < b3, 0.7, 0.3, 0.2 > \}$$

Assume $U = \{p1, p2, p3, p4\}$ exists a universe and R exists an equivalent connection its division of U is expressed as:

$$U/R = \{\{p1, p2\}, p4\}$$

Assume

$$N(F) = \{(p1, (0.3, 0.2, 0.5)), (p2, (0.3, 0.2, 0.5)), (p3, (0.4, 0.5, 0.2))\}.$$

$$\underline{N}(F) = \{(p1, (0.3, 0.2, 0.5)), (p2, (0.3, 0.2, 0.5)), (p3, (0.4, 0.5, 0.2))\}$$

$$\overline{N}(F) = \{(p1, (0.3, 0.2, 0.5)), (p2, (0.3, 0.2, 0.5)), (p3, (0.4, 0.5, 0.2))\}$$

RNSS can estimate the upper and lower estimates for every universe element of U. Each element can exist in one of the partition elements.

4. Experimental Analysis

A. Data Used

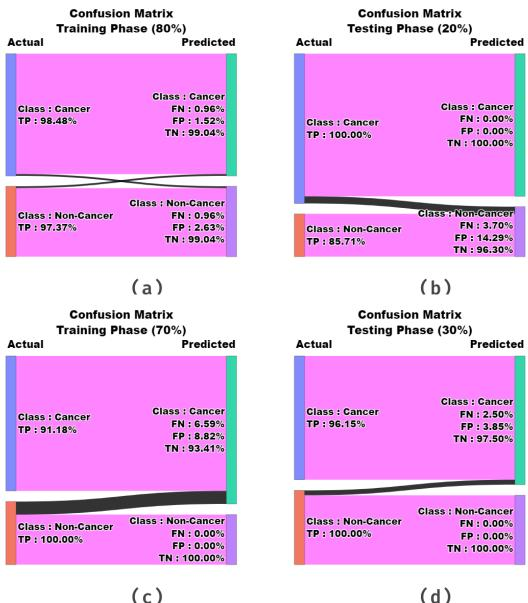
The performance analysis of the BARNSS-OCD approach can be tested using benchmark dataset, which contains 131 samples with two classes as defined in Table 1.

Classes	No. of Instance		
Cancer	87		
Noncancer	44		
Total Instances	131		

Table 1: Details on database

B. Classifier Results on OC Detection

Fig. 3 illustrates the confusion matrices achieved by the BARNSS-OCD methodology at 80%:20% and 70%:30% of TRAS/TESS. The simulation outcome inferred that the BARNSS-OCD algorithm has effective detection of cancer and Noncancer samples in 2 classes.



(c)

Figure 3: Confusion matrices of (a, b) 80% TRAS and 20% TESS and (c, d) 70% TRAS and 30% TESS

In Table 2 and Fig. 4, the recognition results of the BARNSS-OCD technique are given. The results properly recognized the cancer and Noncancer instances. With 80%TRAS, the BARNSS-OCD system gains average accu_v, sens_v, spec_v, F1_{score}, and MCC of 97.93%, 97.93%, 97.93%, 97.93%, and 95.85%, correspondingly. Additionally, with 20% TESS, the BARNSS-OCD algorithm attains average $accu_{y}$, $sens_{y}$, $spec_{y}$, $F1_{score}$, and MCC of 97.93%, 97.93%, 97.93%, 97.93%, and 95.85%, correspondingly.

Table 2: Recognition outcome of BARNSS-OCD system at 80% TRAS and 20% TESS

Classes	Accu _y	Sens _y	Spec _y	F1 _{Score}	MCC
TRAS (80%)					
Cancer	98.48	98.48	97.37	98.48	95.85
Noncancer	97.37	97.37	98.48	97.37	95.85
Average	97.93	97.93	97.93	97.93	95.85
TESS (20%)					
Cancer	95.24	95.24	100.00	97.56	90.35
Noncancer	100.00	100.00	95.24	92.31	90.35
Average	97.62	97.62	97.62	94.93	90.35



Figure 4: Average of BARNSS-OCD system at 80% TRAS and 20% TESS

In Table 3 and Fig. 5, the recognition outcomes of the BARNSS-OCD system are demonstrated. The outcomes appropriately recognized the cancer and Noncancer samples. With 70%TRAS, the BARNSS-OCD system achieves average $accu_y$, $sens_y$, $spec_y$, $F1_{score}$, and MCC of 89.66%, 89.66%, 89.66%, 91.92%, and 85.04%, correspondingly. Besides, with 30%TESS, the BARNSS-OCD methodology reaches average $accu_y$, $sens_y$, $spec_y$, $F1_{score}$, and MCC of 96.67%, 96.67%, 97.30%, and 94.73%, correspondingly.

Table 3: Recognition outcome of BARNSS-OCD system at 70%:30% of TRAS and TESS

Classes	Accuy	Sens _y	Spec _y	F1 _{Score}	MCC	
TRAS (70%)						
Cancer	100.00	100.00	79.31	95.38	85.04	
Noncancer	79.31	79.31	100.00	88.46	85.04	
Average	89.66	89.66	89.66	91.92	85.04	
TESS (30%)						
Cancer	100.00	100.00	93.33	98.04	94.73	
Noncancer	93.33	93.33	100.00	96.55	94.73	
Average	96.67	96.67	96.67	97.30	94.73	

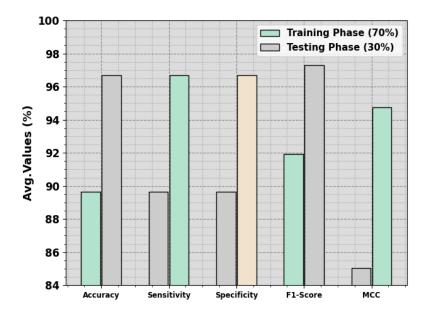


Figure 5: Average of BARNSS-OCD technique under 70% TRAS and 30% TESS

C. Discussion

Table 4 reports a detailed comparison outcome of the BARNSS-OCD system interms of distinct measures [22]. In Fig. 6, a comparative study of the BARNSS-OCD approach in terms of $accu_y$ and $F1_{score}$ are given. The results highlighted that the BARNSS-OCD technique properly recognized the classes. Based on $accu_y$, the BARNSS-OCD technique gains higher $accu_y$ of 97.93% while the OIDCNN-OPMDD, DBN, CNN, Inceptionv4, and DenseNet161 models obtain lower $accu_y$ of 97.50%, 86.36%, 94.14%, 85.14%, and 90.06%, correspondingly.

Table 4: Comparison outcome	of BARNSS-OCD technique	with other DL approaches

Methods	Accu _y	Sens _y	Spec _y	F1 _{Score}
BARNSS-OCD	97.93	97.93	97.93	97.93
OIDCNN-OPMDD	97.50	97.83	97.83	97.46
DBN Algorithm	86.36	84.12	91.15	85.74
CNN Model	94.14	93.93	96.89	95.39
Inceptionv4	85.14	86.68	89.42	87.24
DenseNet161	90.06	88.21	85.59	86.22

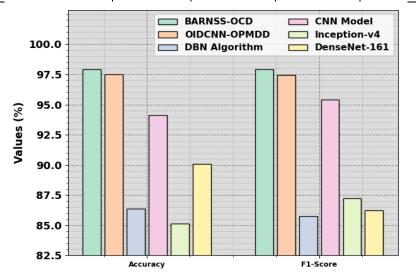


Figure 6: $Accu_y$ and $F1_{score}$ outcome of BARNSS-OCD technique with other DL approaches

Also, based on $F1_{score}$, the BARNSS-OCD algorithm reaches superior $F1_{score}$ of 97.93% while the OIDCNN-OPMDD, DBN, CNN, Inceptionv4, and DenseNet161 approaches obtain minimal $F1_{score}$ of 97.46%, 85.74%, 95.39%, 87.24%, and 86.22%, correspondingly.

In Fig. 7, a comparison outcome of the BARNSS-OCD algorithm interms of $sens_y$ and $spec_y$ are given. The outcome exhibited that the BARNSS-OCD algorithm appropriately recognized the classes. With respect to $sens_y$, the BARNSS-OCD system reaches maximum $sens_y$ of 97.93% while the OIDCNN-OPMDD, DBN, CNN, Inceptionv4, and DenseNet161 methodologies gain lower $sens_y$ of 97.83%, 84.12%, 93.93%, 86.68%, and 88.21%, correspondingly

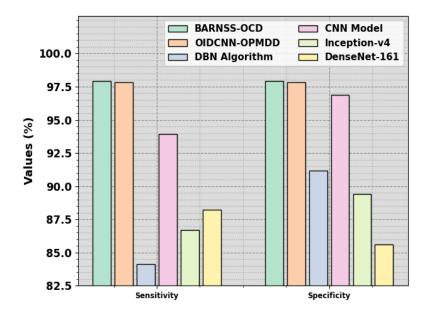


Figure 7: Sensy and specy outcome of BARNSS-OCD technique with other DL approaches

. Likewise, interms of $spec_y$, the BARNSS-OCD method reaches superior $spec_y$ of 97.93% while the OIDCNN-OPMDD, DBN, CNN, Inceptionv4, and DenseNet161 systems gain minimal $spec_y$ of 97.83%, 91.15%, 96.89%, 89.42%, and 85.59%, correspondingly. Therefore, the BARNSS-OCD technique is presented that superior to existing approaches.

5. Conclusion

This paper has presented a novel BARNSS-OCD technique. The objective function of the BARNSS-OCD approach is to utilize DL model for enhanced identification of Oral cancer. It contains four different kinds of procedures namely image preprocessing, DCNN based feature extractor, BA based parameter selection, and RNSS based OC detection. Primarily, the BARNSS-OCD technique takes place the MF is used for image pre-processing and the feature extraction takes place using DCNN model. In addition, BA is used for the hyperparameter selection of the DCNN model. For OC detection process, the BARNSS-OCD technique applies RNSS model. To exhibit the superior efficiency of the BARNSS-OCD technique, a sequence of experiments is involved. The simulation outcomes indicate that the BARNSS-OCD technique gains better performance compared to other DL models.

Funding: "This research received no external funding"

Conflicts of Interest: "The authors declare no conflict of interest."

References

- [1] Jeyaraj, P.; Nadar, E.S. Computer-assisted medical image classification for early diagnosis of oral cancer employing deep learning algorithm. J. Cancer Res. Clin. Oncol. 2019, 145, 829–837.
- [2] Adeoye, J.; Choi, S.W.; Thomson, P. Bayesian disease mapping and The 'high-risk' oral cancer population in Hong Kong. J. Oral Pathol. Med. 2020, 49, 907–913.

- [3] R. Saarumathi, W. Ritha. (2024). A Legitimate Productive Repertoire Replica Betwixt Envirotech Outlay Towards Fragile Commodities Using Trapezoidal Neutrosophic Fuzzy Number. International Journal of Neutrosophic Science, 24 (1), 104-118
- [4] Smarandache F., and Abobala, M., " n-Refined Neutrosophic Vector Spaces", International Journal of Neutrosophic Science, Vol. 7, pp. 47-54, 2020.
- [5] Chu, C.; Lee, N.; Ho, J.; Choi, S.; Thomson, P. Deep learning for clinical image analyses in oral squamous cell carcinoma: A review. JAMA Otolaryngol. Head Neck Surg. 2021, 147, 893–900.
- [6] Tuqa A. H. Al-Tamimi, Luay A. A. Al-Swidi, Ali H. M. Al-Obaidi. "Partner Sets for Generalizations of MultiNeutrosophic Sets." International Journal of Neutrosophic Science, Vol. 24, No. 1, 2024, PP. 08-13
- [7] Parimala, M., Karthika, M. and Smarandache, F., 2020. A review of fuzzy soft topological spaces, intuitionistic fuzzy soft topological spaces and neutrosophic soft topological spaces. International Journal of Neutrosophic Science, Vol. 10, No. 2, 2020 , PP. 96-104.
- [8] Ashraf, S. and Abdullah, S., 2020. Decision support modeling for agriculture land selection based on sine trigonometric single valued neutrosophic information. International Journal of Neutrosophic Science (IJNS), 9(2), pp.60-73.
- [9] Song, B.; Sunny, S.; Li, S.; Gurushanth, K.; Mendonca, P.; Mukhia, N.; Patrick, S.; Gurudath, S.; Raghavan, S.; Tsusennaro, I.; et al. Bayesian deep learning for reliable oral cancer image classification. Biomed. Opt. Express 2021, 12, 6422–6430.
- [10] Song, B.; Li, S.; Sunny, S.; Gurushanth, K.; Mendonca, P.; Mukhia, N.; Patrick, S.; Gurudath, S.; Raghavan, S.; Tsusennaro, I.; et al. Classification of imbalanced oral cancer image data from high-risk population. J. Biomed. Opt. 2021, 26, 105001.
- [11] Mira, E.S., Sapri, A.M.S., Aljehani, R.F., Jambi, B.S., Bashir, T., El-Kenawy, E.S.M. and Saber, M., 2024. Early Diagnosis of Oral Cancer Using Image Processing and Artificial Intelligence. Fusion: Practice and Applications, 14(1), pp.293-308.
- [12] Mohan, R., Rama, A., Raja, R.K., Shaik, M.R., Khan, M., Shaik, B. and Rajinikanth, V., 2023. OralNet: Fused Optimal Deep Features Framework for Oral Squamous Cell Carcinoma Detection. Biomolecules, 13(7), p.1090.
- [13] Huang, Q., Ding, H. and Razmjooy, N., 2024. Oral cancer detection using convolutional neural network optimized by combined seagull optimization algorithm. Biomedical Signal Processing and Control, 87, p.105546.
- [14] Marzouk, R., Alabdulkreem, E., Dhahbi, S., Nour, M.K., Duhayyim, M.A., Othman, M., Hamza, M.A., Motwakel, A., Yaseen, I. and Rizwanullah, M., 2022. Deep Transfer Learning Driven Oral Cancer Detection and Classification Model. Computers, Materials & Continua, 73(2).
- [15] Al Duhayyim, M., Malibari, A., Dhahbi, S., Nour, M.K., Al-Turaiki, I., Obayya, M.I. and Mohamed, A., 2023. Sailfish Optimization with Deep Learning Based Oral Cancer Classification Model. Comput. Syst. Sci. Eng., 45(1), pp.753-767.
- [16] Khan, S.U.R. and Asif, S., 2024. Oral cancer detection using feature-level fusion and novel self-attention mechanisms. Biomedical Signal Processing and Control, 95, p.106437.
- [17] Huang, Q., Ding, H. and Razmjooy, N., 2023. Optimal deep learning neural network using ISSA for diagnosing the oral cancer. Biomedical Signal Processing and Control, 84, p.104749.
- [18] Jana, B.R., Thotakura, H., Baliyan, A., Sankararao, M., Deshmukh, R.G. and Karanam, S.R., 2023. Pixel density based trimmed median filter for removal of noise from surface image. Applied Nanoscience, 13(2), pp.1017-1028.
- [19] Lin, C., Tuo, X., Wu, L., Zhang, G. and Zeng, X., 2024. Accurate Capacity Prediction and Evaluation with Advanced SSA-CNN-BiLSTM Framework for Lithium-Ion Batteries. Batteries, 10(3), p.71.
- [20] Olivares, R., Salinas, O., Ravelo, C., Soto, R. and Crawford, B., 2024. Enhancing the Efficiency of a Cyber SOC Using Biomimetic Algorithms Empowered by Deep Q–Learning.
- [21] Bhutani, K. and Aggarwal, S., 2017. Neutrosophic Rough Soft Set-A Decision Making Approach to Appendicitis Problem. Neutrosophic sets and systems, 16, pp.70-75.
- [22] Alabdan, R., Alruban, A., Hilal, A.M. and Motwakel, A., 2022, December. Artificial-intelligence-based decision making for oral potentially malignant disorder diagnosis in internet of medical things environment. In Healthcare (Vol. 11, No. 1, p. 113). MDPI.